Tellus (1985), *37A*, 41–55

The effect of finite-amplitude baroclinic waves on passive, low-level, atmospheric constituents, with applications to comma cloud evolution

By BARRY SALTZMAN, *Department of Geology and Geophysics, Yale University, New Haven, CT 06511, USA* and CHUNG-MUH TANG, *Universities Space Research Association, The American City Building, Suite 311, Columbia, MD 21044, USA*

(Manuscript received February 10; in final form June 13, 1984)

ABSTRACT

The redistribution of a low-level, passive constituent of the atmosphere under the influence of a growing baroclinic wave is examined by a series of analytical calculations based on a two-level, highly truncated model. It is shown that a constituent confined to the lower half of the atmosphere, and initially homogeneous in the horizontal, will tend to achieve maximum concentration in the low pressure/warm sector portion of the wave and minimum concentration in the high pressure/cold outbreak region with sharpest gradient between the maxima and minima roughly coinciding with the cold front. This distribution is further accentuated if an initial meridional gradient of the constituent exists.

If we assume, as a rough first approximation, that water vapor can be considered to be such a passive constituent, it is shown that the implied relative humidity field and cloud distribution will tend to evolve into the comma-type form commonly observed on satellite images of mid-latitude cyclone waves. Moreover, the solution is shown to replicate the complex flow regime associated with the comma formation, elucidating the dynamical rôles of vertical motion and advection in the cloud evolution.

1. Introduction

One consequence of the motions associated with growing baroclinic waves in middle latitudes is the redistribution of any passive atmospheric constituents (or tracers) that may be present at the time of inception of the waves. We shall investigate this redistribution with the two-level, β-channel, model of the evolution of finite-amplitude baroclinic waves developed previously (for a review see Saltzman and Tang (1982). The fundamental question we pose and discuss is the following: suppose a baroclinic wave forms in a field containing a constituent of horizontally uniform low-level mixing ratio ε, or of zonally uniform meridional gradient ($\partial\varepsilon/\partial y$). To what finite-amplitude distribution will the constituent evolve under the influence of the motions generated by the baroclinic wave?

Secondly, we ask whether the above inferences are consistent with the observed distribution of water vapor and cloud in a baroclinic wave, the latter of which is often characterized by a distinct "comma" form. It will be assumed for this purpose that, as a first-order approximation, we can treat water vapor as such a passive constituent and that we can identify cloud coverage with some critical values of the relative humidity and vertical motion. Although it is clear that a full dynamical description of these cloud and moisture phenomena must depend on more detailed numerical models, it is also of value (at least from a pedagogical viewpoint) to deduce the essentials of the phenomena and its dynamics with the simplest model capable of analytical solution. In fact, one may argue that only from such "minimum" physical models do we gain a true "understanding" of complex phenomena. It is toward this end that this, as well as our previous studies, have been directed. As we shall see, using our simple model it is indeed possible to account qualitatively for many of the main features of the comma cloud dynamics as revealed by detailed synoptic and satellite observations (Carlson, 1980).

2. The model

The symbols to be used in this study are the same as used previously (Saltzman and Tang, hereafter called S-T, 1972, 1975, 1982) and are defined in Appendix A. For present purposes we now add to this list the dependent variable ε, the mixing ratio for an arbitrary constituent of the atmosphere. The full set of basic equations governing the dependent variables ψ (stream function), χ (velocity potential), ω (individual pressure change), and ε are (S-T 1972),

$$\frac{\partial}{\partial t}\nabla^2\psi + V_\psi\cdot\nabla(\nabla^2\psi) + \beta\frac{\partial\psi}{\partial x} - f\frac{\partial\omega}{\partial p} + N = 0, \tag{1}$$

$$f\frac{\partial^2\omega}{\partial p^2} + \frac{\bar{S}}{f}\nabla^2\omega - \frac{\partial}{\partial p}[\mathbf{V}_\psi\cdot\nabla(\nabla^2\psi)] - \beta\frac{\partial^2\psi}{\partial p\,\partial x} + \nabla^2\left[\mathbf{V}_\psi\cdot\nabla\frac{\partial\psi}{\partial p}\right] - P = 0, \tag{2}$$

$$\nabla\cdot\mathbf{V}_\chi + \frac{\partial\omega}{\partial p} = 0, \tag{3}$$

$$\frac{\partial\varepsilon}{\partial t} + \mathbf{V}\cdot\nabla\varepsilon + \omega\frac{\partial\varepsilon}{\partial p} - \mathcal{S}_\varepsilon = 0, \tag{4}$$

where

$$N = \mathbf{V}_\chi\cdot\nabla(\nabla^2\psi) + \beta v_\chi + \omega\frac{\partial}{\partial p}\nabla^2\psi - \nabla^2\psi\frac{\partial\omega}{\partial p} + k\cdot\nabla\omega\frac{\partial\mathbf{V}_\psi}{\partial p},$$

$$P = \left\{\frac{\partial N}{\partial p} - \nabla^2\left[\mathbf{V}_\chi\cdot\nabla\frac{\partial\psi}{\partial p}\right]\right\},$$

$$S = \frac{R}{p}\left(\frac{RT}{c_p p} - \frac{\partial T}{\partial p}\right),$$

$\mathcal{S}_\varepsilon$ = source function for ε.

As in the previous studies we consider the two-layer system portrayed in Fig. 1, applied to a fundamental harmonic region of a β-plane having a meridional width D and zonal extent L (representing the wavelength of maximum baroclinic instability). For simplicity we assume that the constituent is confined only to the lower layer wherein its vertical mean concentration is given by ε_3 and the mean production $\mathcal{S}_\varepsilon$ is assumed to be zero. This would be the case, for example, if ε were constrained to the following vertical distribution,

$$\varepsilon(p) = \begin{cases} 2p_2^{-1}(p-p_2)\,\varepsilon_3 & (p > p_2) \\ 0 & (p \leqslant p_2) \end{cases}$$

corresponding physically to the behavior of a constituent whose initial source is near the surface and whose concentration always decreases markedly with height. The variable ε_3 is, therefore, a measure of the mass of the constituent in the complete vertical column (or, in the special case of water vapor, of the "precipitable water").

Next, we expand each of the dependent variables $\xi = (\psi, \chi, \omega, \varepsilon)$ into a zonal mean part $\bar{\xi}$ (y, t) and an eddy part ξ' (x, y, t), as in S-T (1975), i.e.,

$$\xi = \bar{\xi} + \xi',$$

and further resolve each of these parts into an initial, basic, zonal field denoted by the superscript (0); a primary, quasigeostrophic, field denoted by the superscript (1) (Phillips, 1954); and a second order, non quasi-geostrophic, field denoted by the

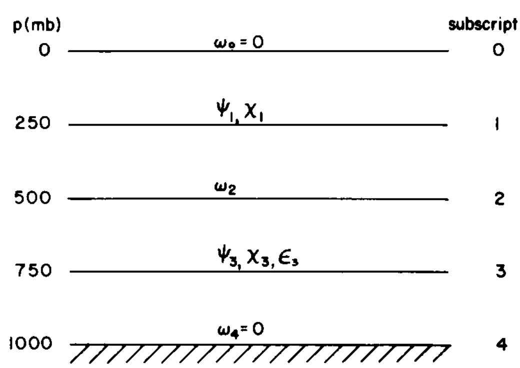

Fig. 1. Two-level model of baroclinic flow as represented by the dependent variables ψ, χ, ω and ε. The pressure levels are shown at the left and the corresponding subscript notation is shown at the right.

superscript (2); i.e.,

$$\bar{\xi} = \bar{\xi}^{(0)} + \bar{\xi}^{(1)} + \bar{\xi}^{(2)},$$

$$\xi' = \xi^{(1)} + \xi^{(2)},$$

so that, e.g., for $\xi = \varepsilon$, we have,

$$\varepsilon = \bar{\varepsilon}^{(0)}(y) + \varepsilon^{(1)}(x, y, t) + \bar{\varepsilon}^{(1)}(y, t) + \varepsilon^{(2)}(x, y, t). \tag{5}$$

We can then derive systems of equations for each of the above components, which will differ from those summarized in S-T (1982) only by the addition of equations for ε. The systems of equations take the following forms:

(I) Equations for the primary wave, $[\psi^{(1)}, \omega^{(1)}, \chi^{(1)}, \varepsilon^{(1)}]$:

$$\frac{\partial}{\partial t} \nabla^2 \psi^{(1)}_{1,3} + \left(\bar{u}^{(0)} \frac{\partial}{\partial x} \nabla^2 \ \psi^{(1)}\right)_{1,3} + \beta \frac{\partial \psi^{(1)}_{1,3}}{\partial x} \mp \frac{f\omega^{(1)}_2}{p_2} = 0, \tag{6a}$$

$$\frac{\tilde{S}}{f} \nabla^2 \omega^{(1)}_2 - \frac{2f}{p_2^2} \omega^{(1)}_2 + \frac{2\beta}{p_2} \frac{\partial \psi^{(1)}_T}{\partial x} + \frac{4}{p_2} \bar{u}^{(0)}_T \frac{\partial}{\partial x} \nabla^2 \psi^{(1)}_2 = 0, \tag{6b}$$

$$\nabla^2 \chi^{(1)}_{1,3} = \mp \frac{\omega^{(1)}_2}{p_2}, \tag{6c}$$

$$\frac{\partial}{\partial t} \varepsilon^{(1)}_3 + \bar{u}^{(0)}_3 \frac{\partial \varepsilon^{(1)}_3}{\partial x} = -\frac{\partial \psi^{(1)}_3}{\partial x} \frac{\partial \bar{\varepsilon}^{(0)}_3}{\partial y} - \bar{\varepsilon}^{(0)}_3 \frac{\omega^{(1)}_2}{p_2}. \tag{6d}$$

(II) Equations for the forced zonal state $[\bar{\psi}^{(1)}, \bar{\omega}^{(1)}, \bar{\chi}^{(1)}, \bar{\varepsilon}^{(1)}]$:

$$\frac{\tilde{S}}{f} \frac{\partial^2 \bar{\omega}^{(1)}_2}{\partial y_2} - \frac{2f}{p_2} \bar{\omega}^{(1)}_2 = A(\psi^{(1)}), \tag{7a}$$

$$\frac{\partial}{\partial t}\left(\frac{\partial^2 \bar{\psi}^{(1)}}{\partial y^2}\right)_{1,3} = -[\mathbf{V}^{(1)}_\psi \cdot \nabla(\nabla^2 \psi^{(1)}]_{1,3} \pm \frac{f}{p_2} \bar{\omega}^{(1)}_2, \tag{7b}$$

$$\frac{\partial^2 \bar{\chi}^{(1)}_{1,3}}{\partial y^2} = \mp \frac{\bar{\omega}^{(1)}_2}{p_2}, \tag{7c}$$

$$\frac{\partial \bar{\varepsilon}^{(1)}_3}{\partial t} = -\frac{\partial}{\partial y} (\overline{v^{(1)}_\psi \varepsilon^{(1)}})_3 - \left(\bar{v}^{(1)}_x \frac{\partial \bar{\varepsilon}^{(0)}}{\partial y}\right)_3 - \bar{\varepsilon}^{(0)}_3 \frac{\bar{\omega}^{(1)}_2}{p_2}. \tag{7d}$$

(III) Equations for the secondary wave fields, $[\psi^{(2)}, \omega^{(2)}, \varepsilon^{(2)}]$:

$$\frac{\partial}{\partial t} \nabla^2 \psi^{(2)}_{1,3} + \left(\bar{u}^{(0)} \frac{\partial}{\partial x} \nabla^2 \psi^{(2)}\right)_{1,3} + \beta \frac{\partial \psi^{(2)}_{1,3}}{\partial x} \mp \frac{f}{p_2} \omega^{(2)}_2 = B(\psi^{(1)}, \omega^{(1)}, \chi^{(1)}; \bar{\psi}^{(1)}, \bar{\omega}^{(1)}, \bar{\chi}^{(1)}), \tag{8a}$$

$$\tilde{S} \nabla^2 \omega^{(2)}_2 - \frac{2f^2}{p_2^2} \omega^{(2)}_2 = C(\psi^{(1)}, \psi^{(2)}, \bar{\psi}^{(1)}), \tag{8b}$$

$$\frac{\partial}{\partial t} \varepsilon^{(2)}_3 + \left(\bar{u}^{(0)} \frac{\partial \varepsilon^{(2)}}{\partial x}\right)_3 = -\left[v^{(1)}_x \frac{\partial \bar{\varepsilon}^{(0)}}{\partial y} + \left(u^{(1)}_x \frac{\partial \varepsilon^{(1)}}{\partial x}\right)' + \left(v^{(1)}_x \frac{\partial \varepsilon^{(1)}}{\partial y}\right)' - \left(\varepsilon^{(1)} \frac{\partial \omega^{(1)}}{\partial p}\right)' + \bar{u}^{(1)}_\psi \frac{\partial \varepsilon^{(1)}}{\partial x} + v^{(1)}_\psi \frac{\partial \bar{\varepsilon}^{(1)}}{\partial y} + v^{(1)}_x \frac{\partial \bar{\varepsilon}^{(1)}}{\partial y} - \bar{\varepsilon}^{(1)} \frac{\partial \omega^{(1)}}{\partial p} + v^{(2)}_\psi \frac{\partial \bar{\varepsilon}^{(0)}}{\partial y} + v^{(2)}_x \frac{\partial \bar{\varepsilon}^{(0)}}{\partial y} - \bar{\varepsilon}^{(0)} \frac{\partial \omega^{(2)}}{\partial p}\right]_3. \tag{8c}$$

Where double signs appear in these equations, the upper sign refers to level 1 (250 mb) and the lower sign to level 3 (750 mb); $\tilde{S}$ is assumed to be a horizontally uniform value of the static stability representative of conditions prevailing near the wave center (i.e., near $y = \frac{1}{2}D$, and A, B, and C represent non-homogeneous forcing due to the lower order fields, the expressions for which are given in S-T (1972, 1975) and are restated in Appendix B in a unified notation. In the present calculations, we approximate C ($=F_g + F_a$, S-T 1975) by including only the linear terms in F_a. We also neglect $\bar{\omega}^{(2)}_2$, which is relatively small over the time span of wave evolution we shall consider (i.e., 5.6 days).

Note that our model still contains many of the deficiencies that were inherent in the previous studies, e.g. (i) the two-level approximation eliminates the possibility for treating the true vertical structure of developing cyclone waves in complete detail, (ii) the latitudinal boundaries are "soft" in the sense that although they are closed for geostrophic (non-divergent) flow, they are open for non-geostrophic (divergent) flow (cf., Moen, 1974; Paegle and MacDonald, 1974), (iii) in treating a single primary wave we neglect barotropic wave-wave, as well as wave-mean flow, interactions and, (iv) no feedbacks to the basic zonal thermal state ($\bar{\psi}^{(0)}$, $\bar{S}^{(0)}$) are included as they were in S-T (1982), so that the primary wave grows exponentially without saturating (i.e., without reaching the occlusion stage) and we can only consider the early stages of wave growth during which the finite-amplitude wave attains its fundamental structure. One consequence of this latter deficiency is that, along with the unabated growth of the amplitude of the motion field, the amplitude of the mixing ratio field ε will also tend to grow beyond realistic bounds. Potentially, this could even lead to nega-

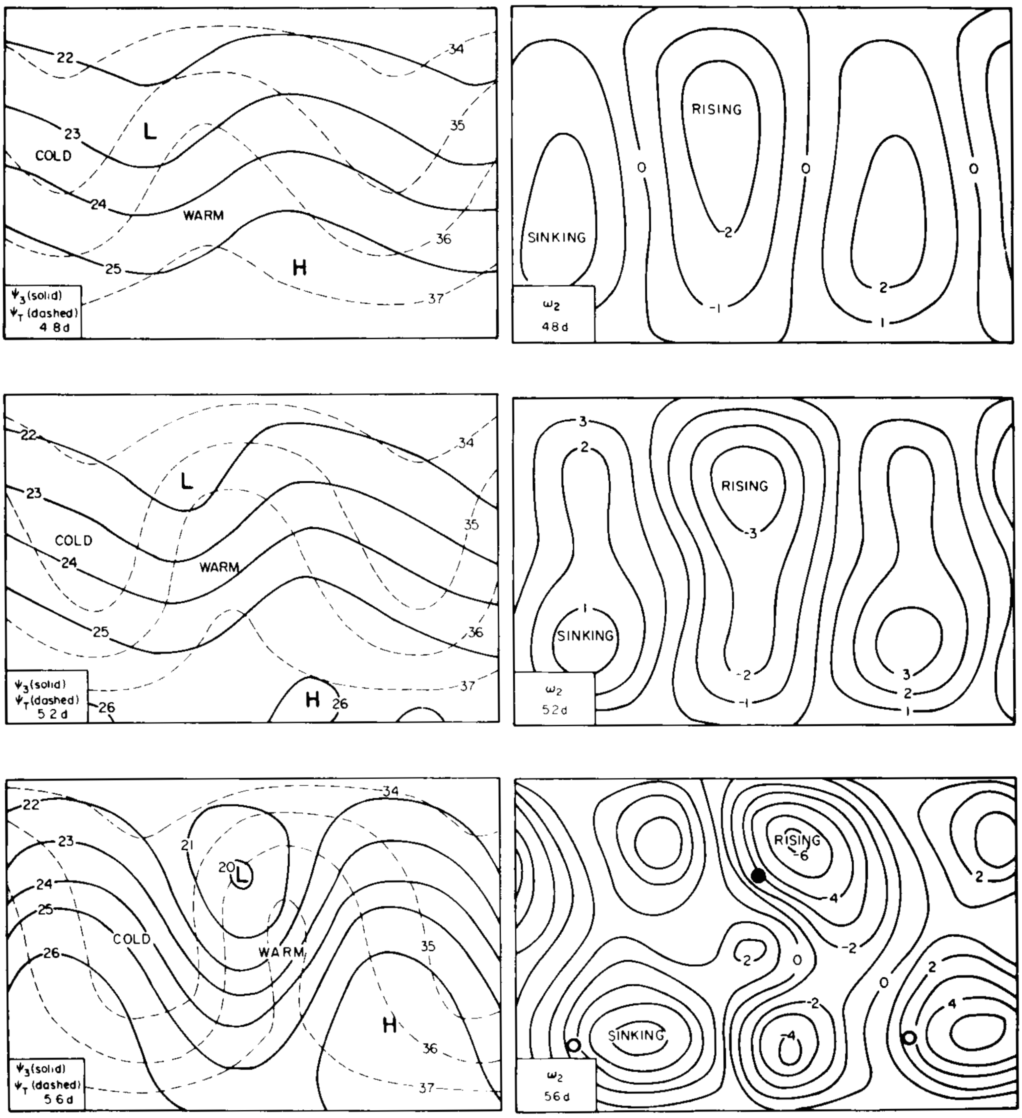

Fig. 2. Solution for fields of ψ_2 and ψ_T in units of 10^7 m^2 s^{-1} (left) and ω_2 in units of 10^{-3} mb s^{-1} (right), at $t = 4.8$, 5.2, and 5.6 days. For $t = 5.6$ days, full and open dots denote closed centers of 750 mb lows and highs, respectively (also shown in Figs. 3, 5 and 6).

tive values of ε_3. For all of these reasons, our results can only be expected to give a qualitative understanding of the rôle of baroclinic, non-geostrophic processes in the early evolution of the wave and its associated constituent concentrations.

3. Solutions for the fields of passive constituents

The analytical solution of (6a, b, c) (7a, b, c) and (8a, b) for the evolution of a baroclinic wave are given in S-T (1972, 1975) and will not be repeated here. In Fig. 2 we plot the solution, corresponding to the same basic state and initial conditions given in S-T (1972), at roughly 10 h intervals for three points in time after the introduction of the initial perturbation: $t = 4.8$, 5.2, and 5.6 days, the last of which (5.6 days) was discussed previously in S-T (1972, Fig. 11a, b; 1975, Fig. 4). According to the solution, the wave progresses eastward at the phase speed $c_r = 16$ m s^{-1}. The analytical solutions of (6d), (7d), and (8c), governing the separate components of ε_3, are given in Appendix C.

Suppose we consider, as Case I, that a non-interacting (passive) constituent, confined to the lower layer, is uniformly distributed horizontally at the time of inception of the wave at $t = 0$ and has an arbitrary mixing ratio, $\bar{\varepsilon}_3^{(0)} = \tilde{\varepsilon}_3^{(0)} = 2 \times 10^{-3}$. In Fig. 3 we show the composite distribution of ε_3 (x, y, t) at $t = 4.8$, 5.2, and 5.6 days obtained by summing the solutions of (6d, 7d, and 8c) given in Appendix C, in accordance with (5).

In Fig. 4 we show the separate components $\varepsilon_3'^{(1)}$, $\bar{\varepsilon}_3^{(1)}$, and $\varepsilon_3^{(2)}$ that comprise the complete field shown in Fig. 3 for $t = 5.6$ days. We can see that the first-order eddy solution $\varepsilon_3'^{(1)}$ alone would give a symmetrical field related to the field of divergence (or, equivalently, of $\omega^{(1)}$, S-T 1972) generated by the first order baroclinic wave. However, the second-order, non-geostrophic processes that become large as the wave evolves lead to a more asymmetric pattern in which the maximum and minimum concentrations are displaced to coincide more closely to the low and high pressure regions, respectively, with a relatively strong gradient between them roughly in the region of the thermal front.

If we consider, as Case II, an initial state in which the constituent is not uniformly distributed, but is characterized by a constant equatorward gradient, $-\partial\bar{\varepsilon}_3^{(0)}/\partial y = +3 \times 10^{-10}$ m^{-1}, the first-order solution will contain a contribution from meridional advection as well as from divergence. In this case, the sequential solution for $t = 4.8$, 5.2, and 5.6 days is of the form shown in Fig. 5. As noted in Section 2, one obvious deficiency of the solution shown in Fig. 5 is that under the influence of the unabated exponential growth of the baro-

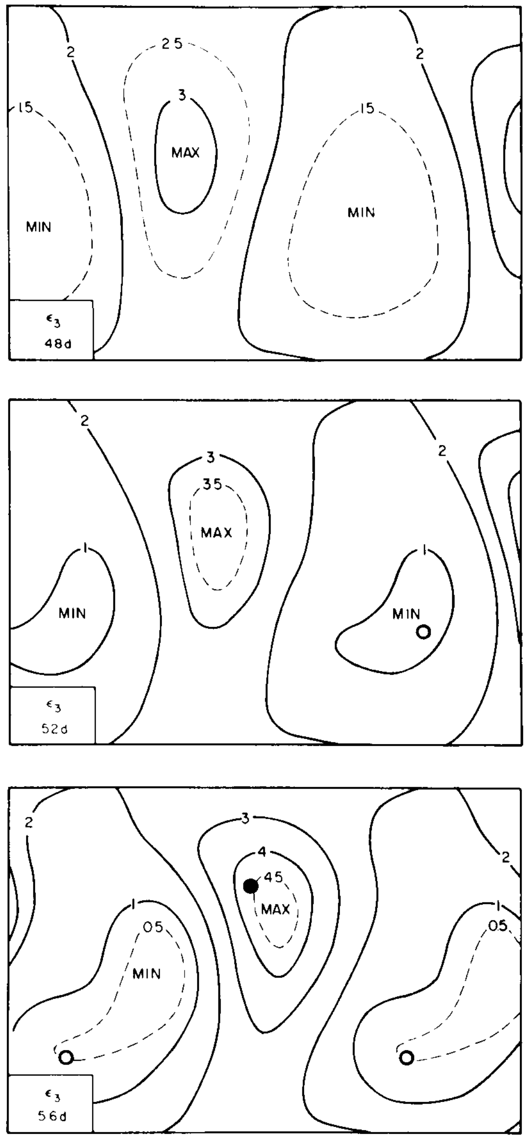

Fig. 3. Solution for field of ε_3 in units of 10^{-3}, for Case I [$\bar{\varepsilon}_3^{(0)} = 2 \times 10^{-3}$ and $\partial\bar{\varepsilon}^{(0)}/\partial y = 0$] at $t = 4.8$, 5.2, and 5.6 days.

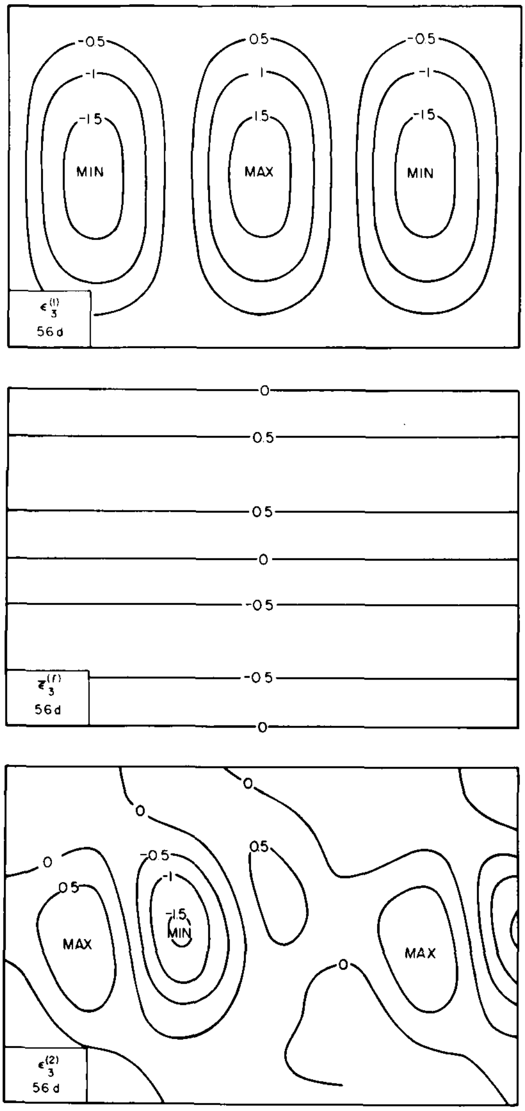

Fig. 4. Component solutions, $\varepsilon_3^{(1)}$, $\bar{\varepsilon}_3^{(1)}$, and $\varepsilon_3^{(2)}$, at 5.6 days, for the complete Case I solution shown in Fig. 3.

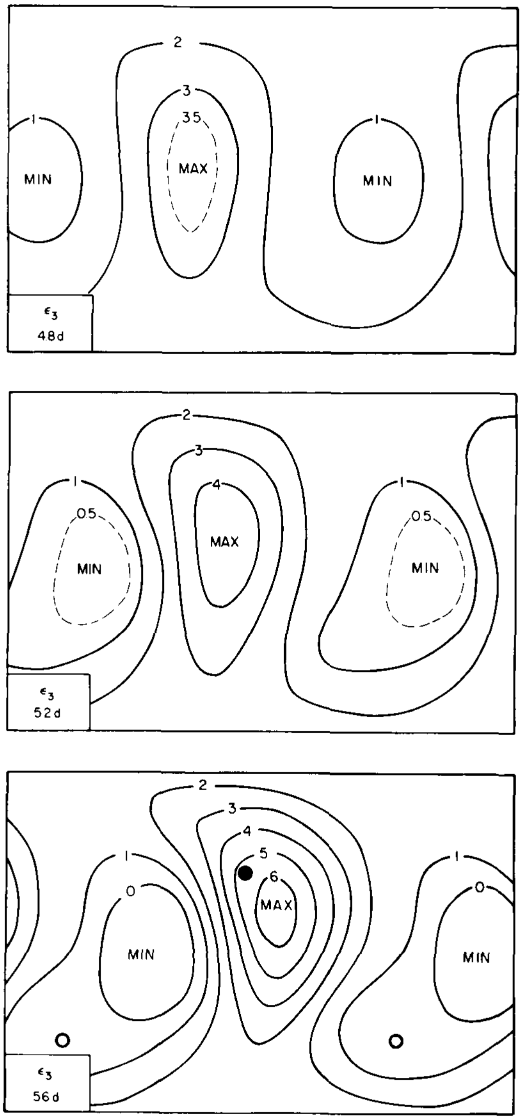

Fig. 5. Solution for field of ε_3 in units of 10^{-3}, for Case II [$\bar{\varepsilon}_3^{(0)} = 2 \times 10^{-3}$ and $\partial\bar{\varepsilon}_3^{(0)}/\partial y = -3 \times 10^{-10}\ \mathrm{m}^{-1}$] at $t =$ 4.8, 5.2, and 5.6 days.

clinic wave, the amplitude of ε also grows at an unrealistic rate so that, depending on the initial mean value of ε, negative values may even be generated. This occurred at $t = 5.6$ days. Although this is physically unacceptable, it is likely that if proper account were taken of wave occlusion processes (e.g., S-T, 1982) this unrealistic feature would be removed without altering the general nature of this solution. Aside from this increase in amplitude, this solution for $\partial\bar{\varepsilon}^{(0)}/\partial y \neq 0$ is similar in form and phase to the solution shown in Fig. 3 for $\partial\bar{\varepsilon}^{(0)}/\partial y = 0$.

4. Inferences concerning water vapor and cloud distribution in baroclinic waves

As is well-known, water vapor is not a "passive" constituent of the atmosphere; condensation and evaporation are continually taking place, and the condensation process entails release of latent heat that can modify the temperature and motion fields of the waves. Nonetheless, we shall assume that these processes are small enough relative to the advective processes that we can neglect them as a first approximation and explore the implications of our solutions for the distributions of water vapor and cloud in baroclinic waves. Thus, if we let $\varepsilon = \varepsilon_v$ (water vapor mixing ratio) we see from Fig. 5 that under the influence of a growing baroclinic wave, an initial "climatological" basic state characterized by $\bar{\varepsilon}^{(0)}_{v3}(\frac{1}{2}D) = 2 \times 10^{-3}$ and $\partial\bar{\varepsilon}^{(0)}_{v3}/\partial y = -3 \times 10^{-10}$ m^{-1} would become eddied into a high concentration pool in the low pressure region and low concentration pool in the high pressure region separated by a strong east-west gradient in the frontal region. Although, for the reasons given previously, we find unrealistic values of the maxima and minima at $t = 5.6$ days, we assume the distributions are qualitatively correct, and can even imagine that the neglected evaporation, condensation, and precipitation processes would at least partially offset these unrealistic maxima and minima. That is, to some degree we can identify supersaturation with the transformation of vapor to liquid water.

With the above limitation in mind, we next obtain from the mixing ratio distribution and the thermal field of the wave (extrapolated to level 3) a qualitative estimate of the field of relative humidity r, defined by

$$r(x, y) = \frac{\varepsilon_{v3}(x, y)}{\varepsilon_{vsat}(T_3(x, y))}, \tag{9}$$

where $T_3 = T_2 + 18K$. For this purpose, we simply set $\varepsilon_v = 0$ where $\varepsilon_v < 0$ and allow r to achieve highly supersaturated values (>100%) where ε_v is large. The patterns of r obtained for $t = 4.8$, 5.2, and 5.6 days are shown in Fig. 6.

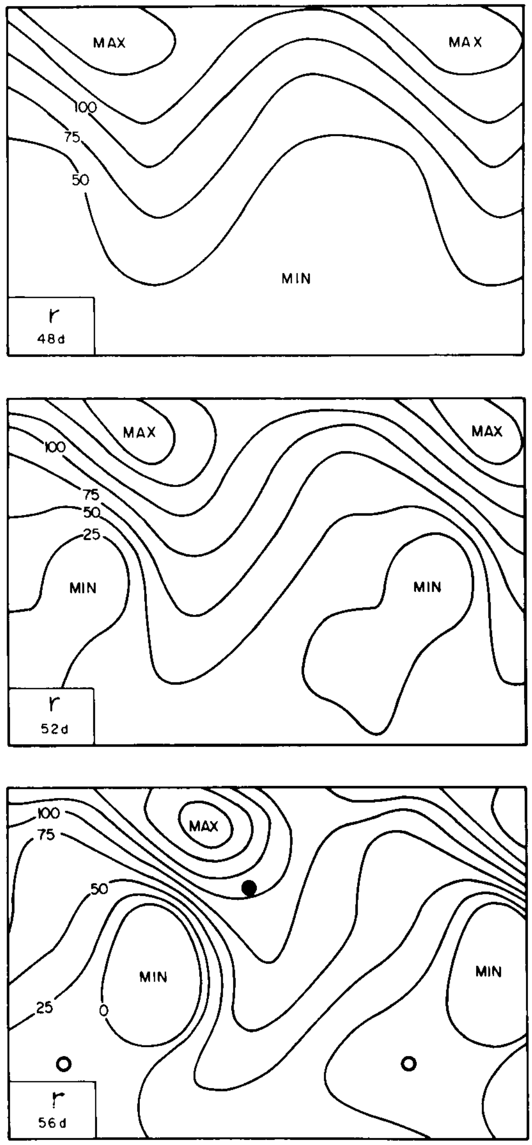

Fig. 6. Field of relative humidity r, in units of %, corresponding to ε_3 fields for Case II shown in Fig. 5, for $t = 4.8$, 5.2, and 5.6 days.

If as in many dynamical models, we assume that cloud amount is proportional to r (e.g., Smagorinsky, 1960; Vallis, 1982); we can see that the solution qualitatively portrays the evolution of the "comma-cloud" structure commonly observed in satellite images of developing mid-latitude cyclones. Further, if as in some other models (Lewis, 1957) we relate cloud coverage to some arbitrary critical values of r *and also* vertical motion ($\sim -\omega_2$), we can obtain cloud distributions that may exhibit even more realistic evolutions to the comma-shape. For example, in Fig. 7 we show the cloud coverage obtained by applying the conditions $r > 0.60$ and $\omega < 0$ to the results shown in Figs. 2 and 6. This sequence can be seen to compare favorably with the schematic cloud evolution sequence in a cyclone wave given by Anderson and Veltishchev (1973, Fig. III.5.5), and with Fig. 8 showing a sequence of GOES infrared

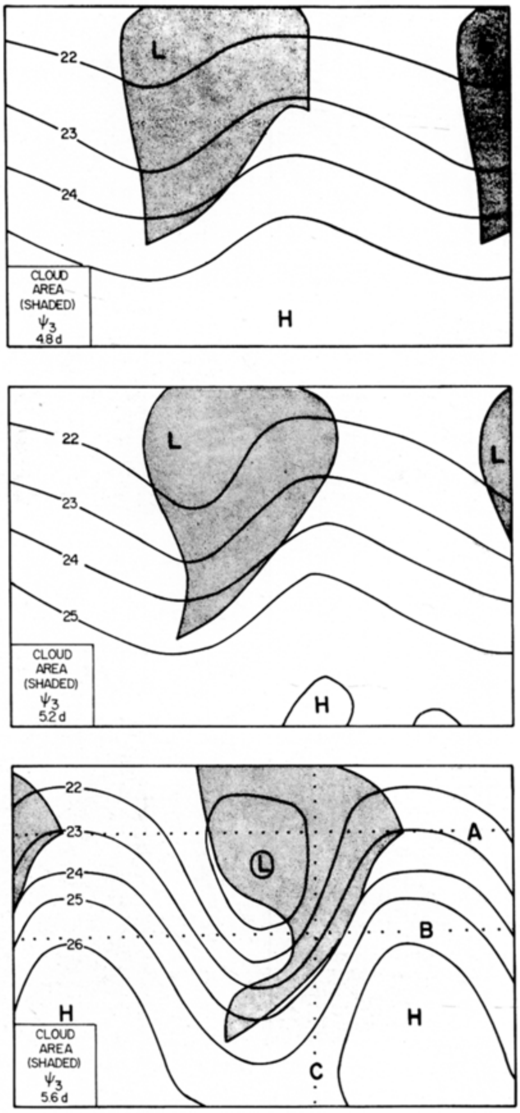

Fig. 7. Cloud areas deduced for Case II from the condition ($r > 0.60$, $\omega < 0$) applied to Fig. 6, for $t = 4.8$, 5.2, and 5.6 days. Dotted lines labeled A, B, and C, for $t = 5.6$ days, are those along which the vertical cross sections shown in Figs. 10, 11, and 12 are drawn.

images spaced roughly 10 h apart (as in our solutions) for a cyclone-wave development over the eastern United States. In the last figure of this GOES sequence (Fig. 8d), the storm is beyond the occlusion stage and is strongly under the influence of non-adiabatic processes over the ocean. The first three images can be roughly compared to the results shown in Fig. 7 for $t = 4.8$, 5.2, and 5.6 days. We note the important rôles played in the comma development at $t = 5.6$ days by the emergence of a strong subsidence region and associated low-level divergence in the region just equatorward of the low-pressure center which generates the dry clear zone (see ω_2, Fig. 2, 5.6 days) and by the horizontal advective processes that sweep water vapor poleward around the low-pressure center at low levels.

An excellent discussion of the synoptic features associated with comma-cloud development has been given by Carlson (1980). His analysis suggests that two main cloud-producing streams of air relative to the moving storm system are involved in the generation of the comma cloud. One is characterized as a potentially-warm "conveyor belt" bringing moist air from the low latitudes, in which middle- and high-level cloud form in the "tail" and eastern portion of the comma; the other is a potentially-cooler low-level "conveyor belt" from the east in which the stratus shield constituting the western portion of the comma forms. In spite of the limitations of our two-level model, these flow features, summarized in Carlson's Figs. 9 and 10 (1980), seem to be well replicated by our solution. The upper and lower level air streams, *relative to our eastward moving baroclinic wave* system containing the qualitative comma cloud, are shown in Fig. 9 (left) along with the satellite infrared cloud image shown in Fig. 8c (right). Also shown in Fig. 9 (left) is the branching of the flow at level 3 (dashed streamline) near the tip of the comma tail, as described by Carlson (1980). In Figs. 10, 11, and 12 we show the vertical cross sections of the solution flow along the three slices labeled A, B, and C in Figs. 7 and 9, including a representation of the variations of temperature and moisture along section C. The low level "cold conveyor" is depicted in section A (Fig. 10); the cold front and adjacent dry-descending and warm-moist-ascending poleward air streams are depicted in section B (Fig. 11); the upper level "warm conveyor" is depicted in the north-south section C (Fig. 12). Although these features emerge naturally in detailed numerical forecasting solutions, we believe the present, two-layer, highly-truncated model is the "minimum" low-order system capable of demonstrating that these complex features follow, qualitatively at least, from the basic laws governing atmospheric behavior.

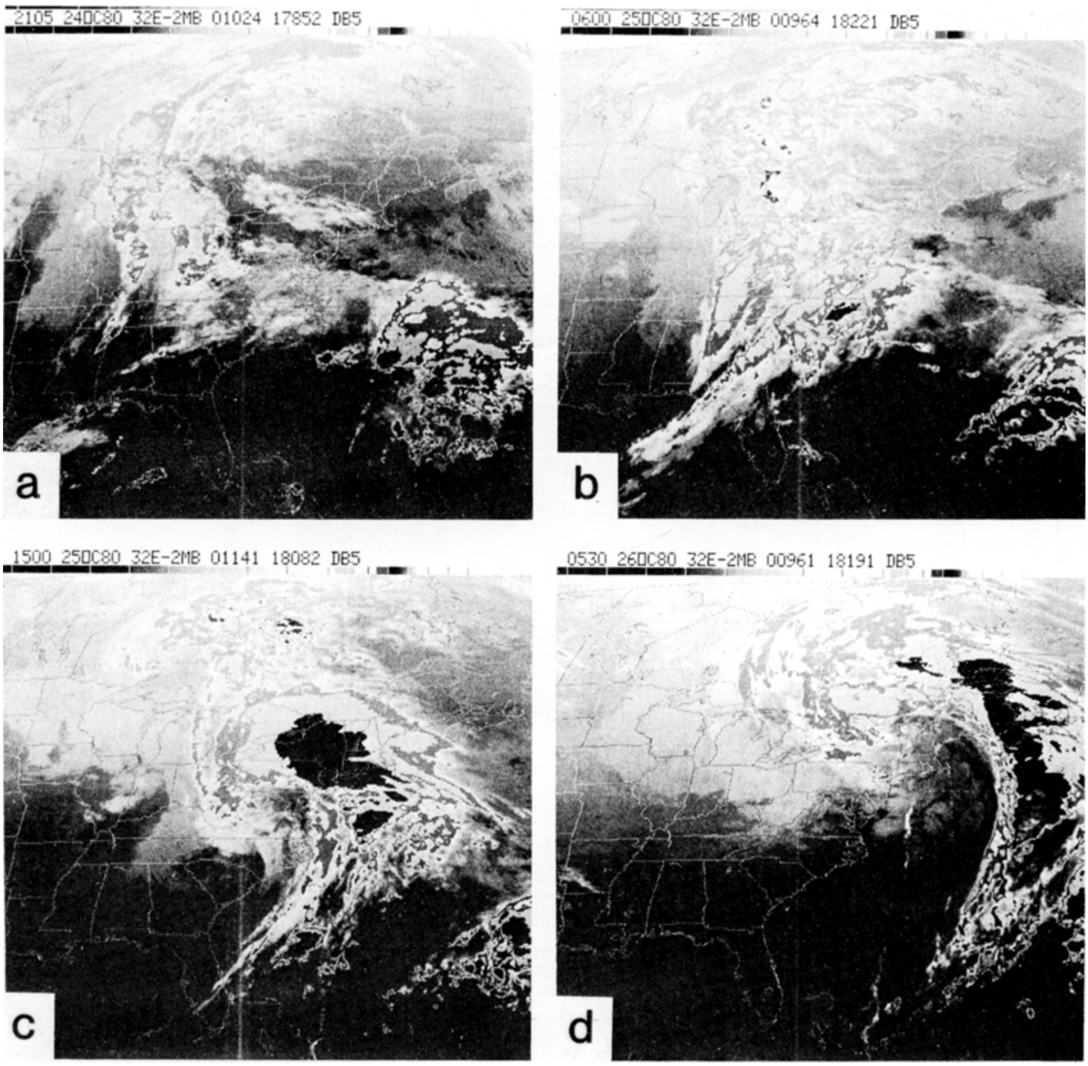

Fig. 8. Sequence of GOES infrared images, spaced roughly 10 h apart, of cloud coverage associated with an evolving cyclone-wave over the eastern United States, (a) 2105 GMT, 24 OCT, (b) 0600 GMT, 25 OCT, (c) 1500 GMT, 25 OCT, (d) 0530 GMT, 26 OCT.

5. Concluding remarks

As we have noted, the present study is meant to complement the more detailed numerical modeling efforts aimed at accounting for and predicting large-scale weather phenomena. It is at least of pedagogical value to be able to show that major observational features can be explained in terms of highly idealized, simple, models that contain a minimum of essential physical ingredients.

In the present case, we have (1) deduced the evolving distribution of an arbitrary low-level passive tracer or pollutant under the influence of a growing baroclinic wave, and (2) applied this solution to show that a two-level, adiabatic, baroclinic model including non-geostrophic, finite-amplitude, passive-advective effects is apparently sufficient to yield a qualitative solution for the mean features and underlying dynamics of comma cloud formation. It is clearly possible and potentially instructive to improve upon our simple model by many further additions short of a full numerical

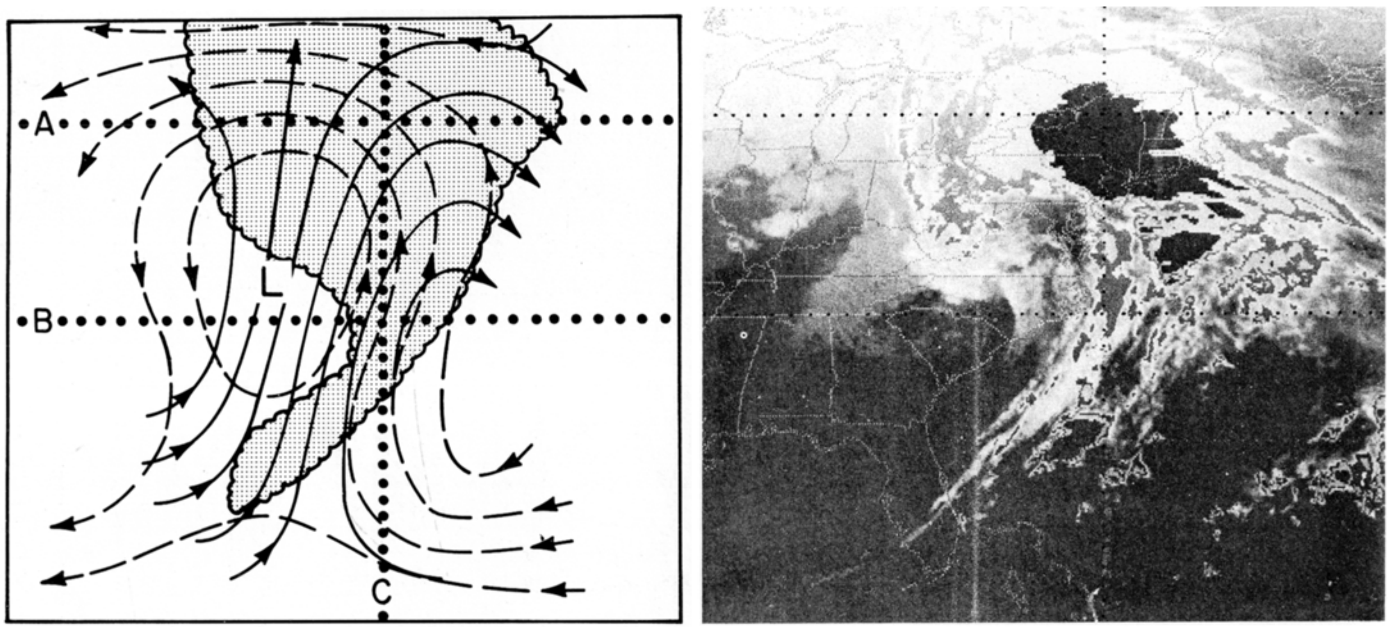

Fig. 9. Left: The solution at 5.6 days showing the level 2 upper streamlines (solid lines) and level 3 lower streamlines (dashed lines), both relative to the *moving* wave, in the vicinity of the comma cloud (scalloped area). Air is rising throughout the comma cloud area. Right: Comparable GOES infrared image of a comma cloud as shown in Fig. 8c. Dotted lines indicate section cross sections shown in Figs. 10, 11, and 12.

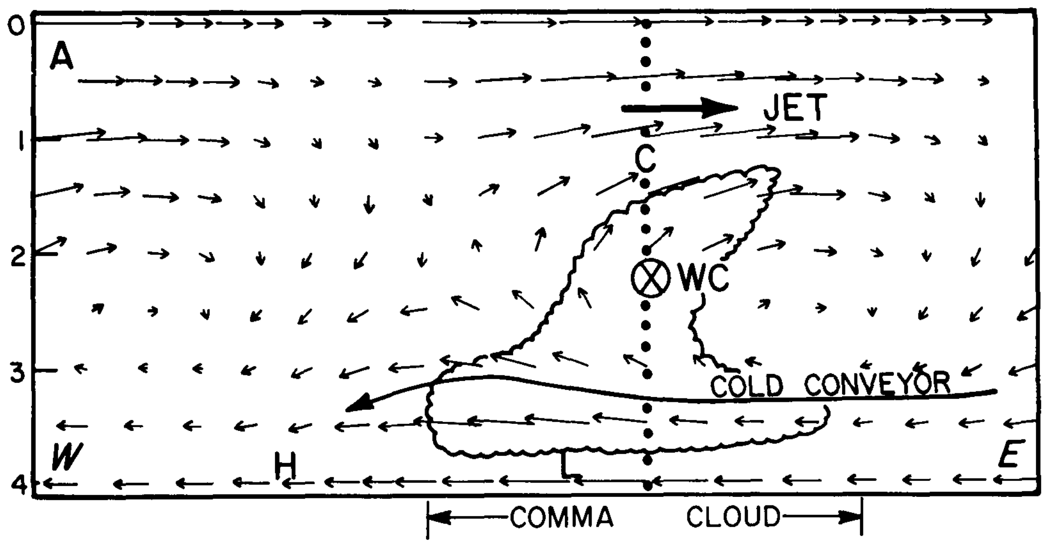

Fig. 10. West-east vertical cross section, (A) of Figs. 7 and 9, across the comma cloud region of the wave poleward of the surface low pressure center, showing the solution vector air motions relative to the eastward moving wave. Note the low-level "cold conveyor", upper-level "jet stream", and "warm conveyor" streamflow (labeled "WC") into the plane along cross section C of Fig. 7. The locations of the surface low and high are indicated by L and H. The comma cloud region is labeled on the abscissa, and a schematic conceptualization of the probable cloud cross section is shown by the scalloped region.

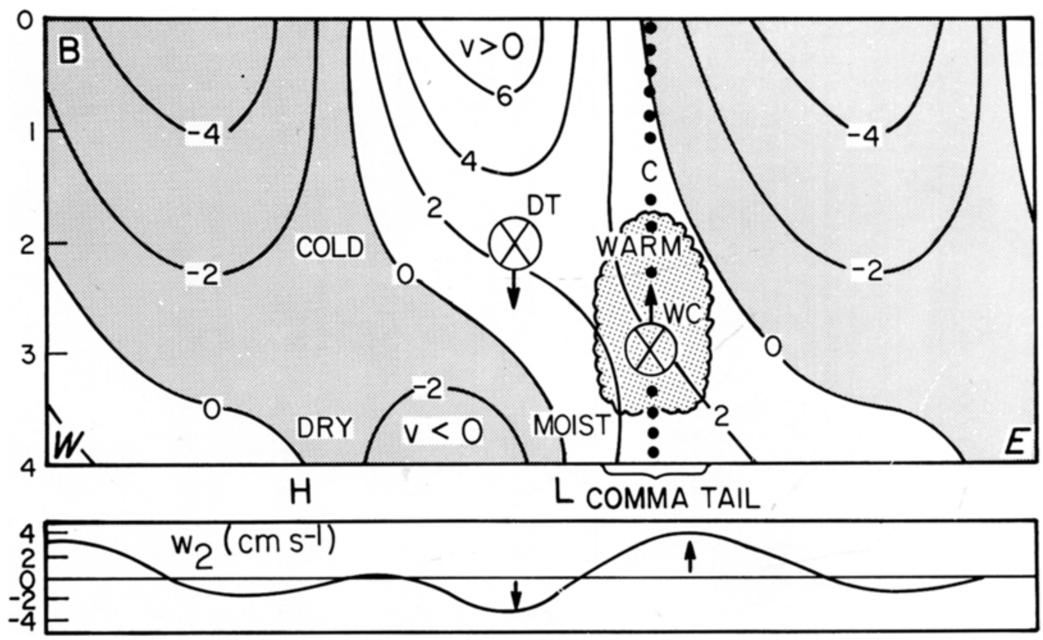

Fig. 11. West-east vertical cross section, (B) of Fig. 9, across the middle latitude of the wave, showing the meridional component of the wind v (in units of 10 m sec^{-1}), the maxima of temperature T and relative humidity r. Note the *high-level* northward-moving "dry tongue", DT, and adjacent *low-level* northward-moving moist warm "conveyor", WC, streamflow paralleling the frontal region. The distribution of vertical motion ω at level 2 is shown in the lower panel.

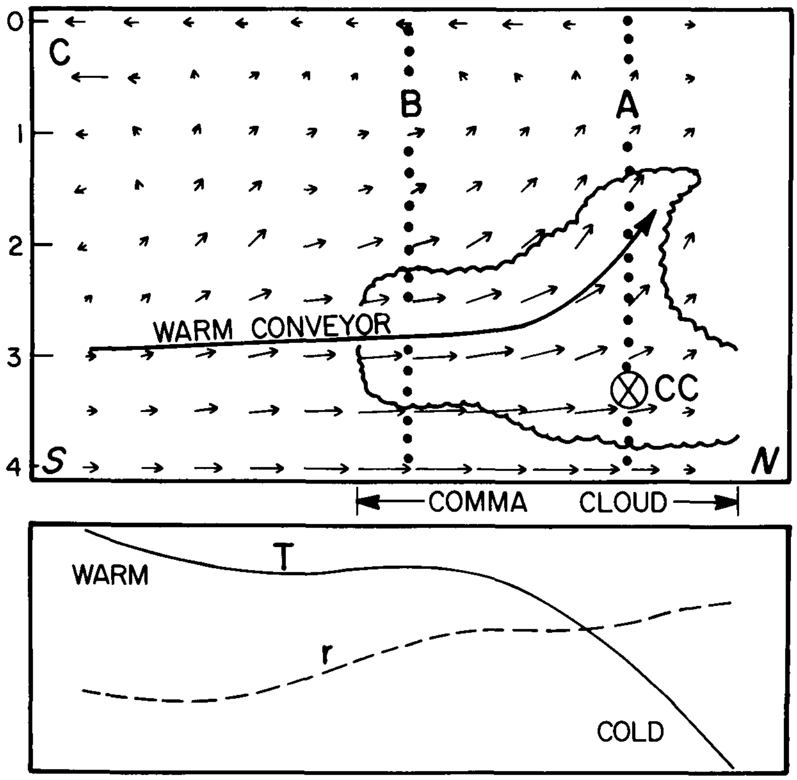

Fig. 12. South-north vertical cross section (C) of Fig. 7, showing the "warm conveyor" flow overriding the east-west "cold conveyor" flow into the plane of the cross section marked by CC. The distributions of T and r along this section are shown in the lower panel. The comma cloud extent is indicated on the abscissa, and a hypothetical cloud cross section is shown by the scalloped region.

treatment. These include additional levels in the vertical, wave-wave and wave-meanflow interactions, wave saturating feedbacks with the basic state, constituent fluxes to and from the upper half of the atmosphere, and the replacement of our semi-empirical model for cloud by simple representations of cloud and precipitation physics including the non-adiabatic effects of latent heat release.

6. Acknowledgments

This study was supported by the National Aeronautics and Space Administration under contract NAS 8-34903 at Yale University and NAS 8-34010 at the Universities Space Research Association.

7. Appendix A

List of symbols

x	distance eastward
y	distance northward
z	height above sea level
p	pressure
t	time
u	eastward wind speed
v	northward wind speed
ω	dp/dt
g	acceleration of gravity
c_p	specific heat at constant pressure
R	gas constant for air
f	Coriolis parameter, $2\Omega \sin \phi$
Ω	angular speed of earth's rotation
ϕ	latitude
β	df/dy

Φ geopotential, gz

ψ geostrophic streamfunction, $f^{-1}\,\Phi$

χ velocity potential

T temperature, $-pfR^{-1}\,\partial\psi/\partial p$

α specific volume

θ potential temperature, $R^{-1}p_4^{\kappa}\,p^{1-\kappa}\,\alpha$

S static stability, $-\alpha\partial\ln\theta/\partial p$

κ R/c_p

$\boldsymbol{i}$ unit vector eastward

$\boldsymbol{j}$ unit vector northward

$\boldsymbol{k}$ unit vector upward

∇ $\boldsymbol{i}\,\partial/\partial x + \boldsymbol{j}\,\partial/\partial y$

$\boldsymbol{V}$ vector horizontal wind, $u\boldsymbol{i} + v\boldsymbol{j} = \boldsymbol{V}_\psi + \boldsymbol{V}_\chi$

$\boldsymbol{V}_\phi$ non-divergent (geostrophic) wind component, $\boldsymbol{k}\times\nabla\psi = u_\psi\boldsymbol{i} + v_\psi\boldsymbol{j}$ ($u_\psi = -\partial\psi/\partial y$, $v_\psi = \partial\psi/\partial x$)

$\boldsymbol{V}_\chi$ irrotational wind component, $\nabla\chi = u_\chi\boldsymbol{i} + v_\chi\boldsymbol{j}$ ($u_\chi = \partial\chi/\partial x$, $v_\chi = \partial\chi/\partial y$)

ζ vertical component of vorticity, $\boldsymbol{k}\cdot\nabla\times\boldsymbol{V} = \nabla^2\psi$

δ horizontal divergence, $\nabla\cdot\boldsymbol{V} = \nabla^2\chi$

and, with reference to Fig. 1, we also define

$$\psi_2 = \tfrac{1}{2}(\psi_1 + \psi_3),$$

$$\psi_T = \tfrac{1}{2}(\psi_1 - \psi_3),$$

$$T = T_2 = \frac{2f}{R}\,\psi_T,$$

$$u_T = -\frac{\partial\psi_T}{\partial y},$$

$$v_T = \frac{\partial\psi_T}{\partial x}.$$

8. Appendix B

Forcing terms in eqs. (7a), (8a) and (8b)

$$A = -\frac{4}{p_2}\left[\overline{\boldsymbol{V}_T^{(1)}\cdot\nabla(\nabla^2\psi_2^{(1)})} - \boldsymbol{k}\cdot\left(\overline{\frac{\partial\boldsymbol{V}_{\psi2}^{(1)}}{\partial x}\times\frac{\partial\boldsymbol{V}_T^{(1)}}{\partial x} + \frac{\partial\boldsymbol{V}_{\psi2}^{(1)}}{\partial y}\times\frac{\partial\boldsymbol{V}_T^{(1)}}{\partial y}}\right)\right],$$

$$\begin{aligned}B = -\Bigg\{&[\boldsymbol{V}_\psi^{(1)}\cdot\nabla(\nabla^2\psi^{(1)})]' + \left[\bar{u}^{(1)}\frac{\partial}{\partial x}\nabla^2\psi^{(1)} + v_\psi^{(1)}\frac{\partial}{\partial y}\left(\frac{\partial^2\bar{\psi}^{(1)}}{\partial y^2}\right)\right] + \left(\beta v_\chi^{(1)} - \frac{\partial\omega^{(1)}}{\partial y}\frac{\partial\bar{u}^{(0)}}{\partial p}\right)\\
&+ \Bigg[\boldsymbol{V}_\chi^{(1)}\cdot\nabla(\nabla^2\psi^{(1)}) + \omega^{(1)}\frac{\partial}{\partial p}\nabla^2\psi^{(1)} - \nabla^2\psi^{(1)}\frac{\partial\omega^{(1)}}{\partial p} - \left(\frac{\partial\omega^{(1)}}{\partial y}\frac{\partial u_\psi^{(1)}}{\partial p} - \frac{\partial\omega^{(1)}}{\partial x}\frac{\partial v_\psi^{(1)}}{\partial p}\right)\Bigg]'\\
&+ \Bigg[\bar{v}_\chi^{(1)}\frac{\partial}{\partial y}\nabla^2\psi^{(1)} + v_\chi^{(1)}\frac{\partial}{\partial y}\left(\frac{\partial^2\bar{\psi}^{(1)}}{\partial y^2}\right) + \bar{\omega}^{(1)}\frac{\partial}{\partial p}\nabla^2\psi^{(1)} + \omega^{(1)}\frac{\partial}{\partial p}\left(\frac{\partial^2\bar{\psi}^{(1)}}{\partial y^2}\right) - \frac{\partial^2\bar{\psi}^{(1)}}{\partial y^2}\frac{\partial\omega^{(1)}}{\partial p}\\
&- \nabla^2\psi^{(1)}\frac{\partial\bar{\omega}^{(1)}}{\partial p} - \frac{\partial\omega^{(1)}}{\partial y}\frac{\partial\bar{u}^{(1)}}{\partial p} - \frac{\partial\bar{\omega}^{(1)}}{\partial y}\frac{\partial u_\psi^{(1)}}{\partial p} + \frac{\partial\omega^{(1)}}{\partial x}\frac{\partial\bar{v}^{(1)}}{\partial p}\Bigg]\Bigg\}_{1,3},\end{aligned}$$

$$C = \frac{4f}{p_2}\left(\frac{\partial\bar{\psi}_T^{(1)}}{\partial y}\frac{\partial}{\partial x}\nabla^2\psi_2^{(1)} + \frac{\partial^2\psi_2^{(1)}}{\partial x\,\partial y}\frac{\partial^2\bar{\psi}_T^{(1)}}{\partial y^2}\right) - \frac{2f}{p_2}\left(\beta\frac{\partial\psi_T^{(2)}}{\partial x} + 2\bar{u}_T^{(0)}\frac{\partial}{\partial x}\nabla^2\psi_2^{(2)}\right).$$

9. Appendix C

Solution for the mixing ratio ε_3

Using the same notation employed in S-T (1972, 1975, 1982), the solutions of (6d), (7d), and (8c) for the components of $\varepsilon_3(x, y, t)$ represented by the expansion (1) can be expressed in the following forms, respectively:

$$\varepsilon_3^{(1)}(x, y, t) = (E_r\cos kX - E_i\sin kX)\sin ly\cdot e^{\nu t} \tag{C1}$$

$$\bar{\varepsilon}_3^{(1)}(y, t) = (G_r\cos 2ly - G_i\sin 2ly)\,e^{2\nu t}, \tag{C2}$$

$$\begin{aligned}\varepsilon_3^{(2)} = \sum_m\sum_n\sum_p\{&[\Upsilon_r(m, n, p)\cos mly + \Pi_r(m, n, p)\\
&\times\sin mly]\cos nkX + [\Upsilon_i(m, n, p)\cos mly\\
&+ \Pi_i(m, n, p)\sin mly]\sin nkX\}\,e^{p\nu\tau}\end{aligned} \tag{C3}$$

To save space, the coefficients in (C1), (C2) and (C3) can be written in terms of a generalized notation, whereby paired relations of the form

$$Z_r = -A + B_r + C_i + D\cdot a,$$

$$Z_i = +A - B_i + C_r + D\cdot b,$$

are condensed to the single relation

$$Z_{r,i} = \mp A \pm B_{r,i} + C_{i,r} + D(a, b),$$

and where the following definitions are introduced,

$$U \equiv \bar{u}_3^{(0)} - c_r,$$

$$V^2 \equiv U^2 + c_i^2,$$

$$W^2 \equiv U^2 + 9c_i^2,$$

$$\bar{\varepsilon}_y^{(0)} \equiv (\partial \bar{\varepsilon}^{(0)}/\partial y)_3,$$

$$\Psi_3 \equiv \Psi_2 - \Psi_T,$$

$$\Lambda \equiv \frac{fl^2 |\Psi_2|^2}{2\bar{u}_T^{(0)}(2Sl^2 p_2^2 + f^2)}.$$

As noted, all other quantities are as defined in S-T (1972, 1975, 1982). Thus, the coefficients in (C1), (C2) and (C3) can be written in the following forms,

$$E_{r,i} = V^{-2}\left[-U\left(\bar{\varepsilon}_y^{(0)} \Psi_{3r,i} \pm \frac{\bar{\varepsilon}_3^{(0)}}{kp_2} \Omega_{i,r}\right) \pm c_i \left(\bar{\varepsilon}_y^{(0)} \Psi_{3i,r} \mp \frac{\bar{\varepsilon}_3^{(0)}}{kp_2} \Omega_{r,i}\right)\right],$$

$$G_r = \Lambda \bar{\varepsilon}_y^{(0)},$$

$$G_i = -\left[2l\Lambda \bar{\varepsilon}^{(0)} - \frac{l}{4c_i}(E_r \Psi_{3i} - E_i \Psi_{3r})\right].$$

The only coefficients appearing in the expansion (C3) for $\varepsilon_3^{(2)}$ are of dimensionality (1, 1, 1), (0, 2, 2), (2, 2, 2), (1, 1, 3), and (3, 1, 3), that is,

$$\Upsilon_{r,i}(1, 1, 1) = \pm E_{r,i}^{(a)} \pm E_{r,i}^{(e1)},$$

$$\Pi_{r,i}(1, 1, 1) = \pm E_{r,i}^{(e2)},$$

$$\Upsilon_{r,i}(0, 2, 2) = \pm E_{r,i}^{(b)} \pm E_{r,i}^{(f3)},$$

$$\Pi_{r,i}(0, 2, 2) = 0,$$

$$\Upsilon_{r,i}(2, 2, 2) = \pm E_{r,i}^{(f1)} \mp \frac{\mu^2}{k^2} E_{r,i}^{(b)},$$

$$\Pi_{r,i}(2, 2, 2) = \pm E_{r,i}^{(f2)},$$

$$\Upsilon_{r,i}(1, 1, 3) = \mp E_{r,i}^{(c1)} \pm E_{r,i}^{(d2)} \pm E_{r,i}^{(g2)},$$

$$\Pi_{r,i}(1, 1, 3) = \mp E_{r,i}^{(c2)} \pm E_{r,i}^{(d4)} \pm E_{r,i}^{(g4)},$$

$$\Upsilon_{r,i}(3, 1, 3) = \pm E_{r,i}^{(c1)} \pm E_{r,i}^{(d1)} \pm E_{r,i}^{(g1)},$$

$$\Pi_{r,i}(3, 1, 3) = \pm E_{r,i}^{(c2)} \pm E_{r,i}^{(d3)} \pm E_{r,i}^{(g3)},$$

where

$$E_{r,i}^{(a)} = \frac{l\bar{\varepsilon}_y^{(0)}}{kp_2 \mu^2 V^2}(c_i \Omega_{r,i} \pm U\Omega_{i,r}),$$

$$E_{r,i}^{(b)} = \frac{-k}{4p_2 \mu^2 V^2}[c_i(\Omega_r E_{r,i} - \Omega_i E_{i,r}) \pm U(\Omega_r E_{i,r} - \Omega_i E_{r,i})],$$

$$E_{r,i}^{(c1)} = \pm \Lambda l \bar{\varepsilon}_y^{(0)} W^{-2}(3c_i \Psi_{3i,r} \mp U\Psi_{3r,i}),$$

$$E_{r,i}^{(c2)} = 2\Lambda W^{-2}[-3c_i(4^{-1}fE_{i,r} + l^2 \Psi_{3i,r} \bar{\varepsilon}_3^{(0)}) + U(4^{-1}fE_{r,i} + l^2 \Psi_{3r,i} \bar{\varepsilon}_3^{(0)})] \mp \frac{l^2}{4c_i W^2}[(E_r \Psi_{3i} - E_i \Psi_{3r})(3c_i \Psi_{3i,r} \mp U\Psi_{3r,i})],$$

$$E_{r,i}^{(d1)} = \left[-2\Lambda \bar{\varepsilon}_3^{(0)} + \frac{1}{4c_i}(E_r \Psi_{3i} - E_i \Psi_{3r})\right]\frac{l}{p_2} \times \left(\frac{2l^2 + \mu^2}{2\mu^2}\right)\frac{(3c_i \Omega_{r,i} \pm U\Omega_{i,r})}{kW^2},$$

$$E_{r,i}^{(d2)} = \left(\frac{2l^2 - \mu^2}{2l^2 + \mu^2}\right) E_{r,i}^{(d1)},$$

$$E_{r,i}^{(d3)} = -\frac{\Lambda \bar{\varepsilon}_y^{(0)}}{kp_2 W^2}\left(\frac{2l^2 + \mu^2}{2\mu^2}\right)(3c_i \Omega_{r,i} \pm U\Omega_{i,r}),$$

$$E_{r,i}^{(d4)} = \left(\frac{2l^2 - \mu^2}{2l^2 + \mu^2}\right) E_{r,i}^{(d3)},$$

$$E_{r,i}^{(e1)} = -V^{-2}\{-c_i[-(\mathscr{B}_3, -\mathscr{A}_3)\bar{\varepsilon}_y^{(0)} - (kp_2)^{-1}\bar{\varepsilon}_3^{(0)} \times (S_a^*(1, 1, 1), Q_a^*(1, 1, 1))] + U[(\mathscr{A}_3, -\mathscr{B}_3)\bar{\varepsilon}_y^{(0)} - (kp_2)^{-1}\bar{\varepsilon}_3^{(0)}(Q_a^*(1, 1, 1), S_a^*(1, 1, 1))]\},$$

$$E_{r,i}^{(e2)} = -V^{-2}[c_i l(kp_2 \mu^2)^{-1}\bar{\varepsilon}_y^{(0)} \times (S_a^*(1, 1, 1), -Q_a^*(1, 1, 1)) - Ul(kp_2 \mu^2)^{-1}\bar{\varepsilon}_y^{(0)} \times (Q_a^*(1, 1, 1), S_a^*(1, 1, 1))],$$

$$E_{r,i}^{(f1)} = -V^{-2}\{\mp c_i[k^2(-\mathscr{D}_3, \mathscr{C}_3)\bar{\varepsilon}_y^{(0)} - (2kp_2)^{-1}\bar{\varepsilon}_3^{(0)} \times (S_a^*(2, 2, 2), Q_a^*(2, 2, 2))] + U[k^2(\mathscr{C}_3, -\mathscr{D}_3)\bar{\varepsilon}_y^{(0)} - (2kp_2)^{-1}\bar{\varepsilon}_3^{(0)} \times (Q_a^*(2, 2, 2), S_a^*(2, 2, 2))]\},$$

$$E_{r,i}^{(f2)} = -V^{-2}[\pm c_i l(4kp_2 \mu^2)^{-1}\bar{\varepsilon}_y^{(0)} - \times (S_a^*(2, 2, 2), Q_a^*(2, 2, 2)) - Ul(4kp_2 \mu^2)^{-1}\bar{\varepsilon}_y^{(0)} \times (Q_a^*(2, 2, 2), S_a^*(2, 2, 2))],$$

$$E_{r,i}^{(f3)} = -V^{-2}\{\mp c_i[\mu^2(\mathcal{F}_3, -\mathcal{E}_3)\,\bar{\varepsilon}_y^{(0)} + (2kp_2)^{-1}\,\bar{\varepsilon}_3^{(0)}$$
$$\times (S_a^*(0, 2, 2), Q_a^*(0, 2, 2))] + U[\mu^2(-\mathcal{E}_3, \mathcal{F}_3)$$
$$\times\,\bar{\varepsilon}_y^{(0)} + (2kp_2)^{-1}\,\bar{\varepsilon}_3^{(0)}\,(Q_a^*(0, 2, 2), S_a^*(0, 2, 2))]\}.$$

$$E_{r,i}^{(g,n)} = -W^{-2}\{\mp 3c_i\,[\alpha_{r,i}(1, n)\,\bar{\varepsilon}_y^{(0)} + (kp_2)^{-1}$$
$$\times (\delta(n)\,\bar{\varepsilon}_y^{(0)}\,\alpha_{r,i}(2, n) - \bar{\varepsilon}_3^{(0)}\,\alpha_{r,i}(3, n))]$$
$$+ U[\bar{\varepsilon}_y^{(0)}\,\alpha_{r,i}(4, n) + (kp_2)^{-1}\,(\delta(n)\,\bar{\varepsilon}_y^{(0)}\,\alpha_{r,i}(5, n)$$
$$- \bar{\varepsilon}_3^{(0)}\,\alpha_{r,i}(6, n))]\},(n = 1, 2, 3, 4).$$

In the above expression for $E_{r,i}^{(g,n)}$, the quantities $\delta(n)$ and $\alpha_{r,i}$ (1–6, n) are defined as follows, with the subscripts (r, i) deleted:

$$\delta(n) = \begin{cases} 3l/(k^2 + 9l^2), & n = 1, 3 \\ l/(k^2 + l^2) & n = 2, 4, \end{cases}$$

$$\alpha(1, 1) = (-\mathcal{M}_3, \mathcal{K}_3),$$

$$\alpha(2, 1) = [(R_a^*(3, 1, 3) + R_g(3, 1, 3)), (P_a^*(3, 1, 3) + P_g(3, 1, 3))],$$

$$\alpha(3, 1) = [S_a^*(3, 1, 3), Q_a^*(3, 1, 3)],$$

$$\alpha(4, 1) = (\mathcal{K}_3, -\mathcal{M}_3),$$

$$\alpha(5, 1) = [(P_a^*(3, 1, 3) + P_g(3, 1, 3), (R_a^*(3, 1, 3) + R_g(3, 1, 3))],$$

$$\alpha(6, 1) = [Q_a^*(3, 1, 3), S_a^*(3, 1, 3)],$$

$$\alpha(1, 2) = (-\mathcal{N}_3, \mathcal{L}_3),$$

$$\alpha(2, 2) = [(R_a^*(1, 1, 3) + R_g(1, 1, 3)), (P_a^*(1, 1, 3) + P_g(1, 1, 3))].$$

$$\alpha(3, 2) = [S_a^*(1, 1, 3), Q_a^*(1, 1, 3)],$$

$$\alpha(4, 2) = (\mathcal{L}_3, -\mathcal{N}_3),$$

$$\alpha(5, 2) = [(P_a^*(1, 1, 3) + P_g(1, 1, 3)), (R_a^*(1, 1, 3) + R_g(1, 1, 3))],$$

$$\alpha(6, 2) = [Q_a^*(1, 1, 3), S_a^*(1, 1, 3)],$$

$$\alpha(1, 3) = (-\mathcal{J}_3, \mathcal{G}_3),$$

$$\alpha(2, 3) = -\alpha(3, 1),$$

$$\alpha(3, 3) = \alpha(2, 1),$$

$$\alpha(4, 3) = (\mathcal{G}_3, -\mathcal{J}_3),$$

$$\alpha(5, 3) = -\alpha(6, 1),$$

$$\alpha(6, 3) = \alpha(5, 1),$$

$$\alpha(1, 4) = (-\mathcal{T}_3, \mathcal{W}_3),$$

$$\alpha(2, 4) = -\alpha(3, 2),$$

$$\alpha(3, 4) = \alpha(2, 2),$$

$$\alpha(4, 4) = (\mathcal{W}_3, -\mathcal{T}_3),$$

$$\alpha(5, 4) = -\alpha(6, 2),$$

$$\alpha(6, 4) = \alpha(5, 2).$$

The quantities P_a^*, Q_a^*, R_a^*, and S_a^* are equal to the quantities P_a, Q_a, R_a, and S_a, respectively, given in Table 2 of S-T (1975), minus the non-linear (quadratic) terms).

REFERENCES

Anderson, R. K. and Veltishchev, N. F. 1973. The use of satellite pictures in weather analysis and forecasting, *Tech. Note No. 124*, World Meteor. Org., Geneva, 275 pp.

Carlson, T. N. 1980. Airflow through mid-latitude cyclones and the comma cloud pattern. *Mon. Wea. Rev. 108*, 1498–1509.

Lewis, W. 1957. Forecasting 700 mb dewpoint depression by a 3-dimensional trajectory technique. *Mon. Wea. Rev. 85*, 297–301.

Moen, L. 1974. A spectral model for investigation of amplifying baroclinic waves. *Tellus 26*, 424–443.

Paegle, J. N. and MacDonald, A. E. 1974. Short numerical integrations of a three-level spectral quasi-geostrophic model. *Mon. Wea. Rev. 102*, 772–783.

Phillips, N. 1954. Energy transformations and meridional circulations associated with simple baroclinic waves in a two-level, quasi-geostrophic model. *Tellus 6*, 273–286.

Saltzman, B. and Tang, C.-M. 1972. Analytical study of the evolution of an amplifying baroclinic wave. *J. Atmos. Sci. 29*, 427–444.

Saltzman, B. and Tang, C.-M. 1975. Analytical study of the evolution of an amplifying baroclinic wave: Part II. Vertical motions and transport properties. *J. Atmos. Sci. 32*, 243–259.

Saltzman, B. and Tang, C.-M. 1982. A review of some analytical studies of finite-amplitude baroclinic waves, including a new algorithm for the saturation effects of static stability and baroclinicity variations. *J. Meteorol. Soc. Japan 60*, 1–14.

Smagorinsky, J. 1960. On the dynamical prediction of large-scale condensation by numerical methods. *Geophys. Monogr. 5*, Am. Geophys. Union, 71–78.

Vallis, G. K. 1982. A statistical-dynamical climate model with a simple hydrology cycle. *Tellus 34*, 211–227.